

Compartment- and context-specific changes in tissue-type plasminogen activator (tPA) activity following brain injury and pharmacological stimulation

Maithili Sashindranath^{1,*}, Andre Laval Samson^{1,*}, Catherine Eliza Downes², Peter John Crack², Andrew John Lawrence^{3,4}, Qiao-Xin Li^{5,6}, Ashley Quan Ping Ng⁷, Nigel Charles Jones⁷, Jessica Jade Farrugia¹, Eman Abdella¹, Jean-Dominique Vassalli⁸, Rime Madani⁸ and Robert Lindsay Medcalf¹

Tissue-type plasminogen activator (tPA) is a major protease of the central nervous system. Most studies to date have used *in situ*- or gel-based zymographic assays to monitor *in vivo* changes in neural tPA activity. In this study, we demonstrate that the amidolytic assay can be adapted to accurately detect changes in net tPA activity in mouse brain tissues. Using the amidolytic assay, we examined differences in net tPA activity in the cerebral cortex, sub-cortical structures and cerebellum in wildtype (WT) and tPA^{-/-} mice, and in transgenic mice selectively overexpressing tPA in neurons. In addition, we assessed changes in endogenous net tPA activity in WT mice following morphine administration, epileptic seizures, traumatic brain injury and ischaemic stroke—neurological settings in which tPA has a known functional role. Under these conditions, acute and compartment-specific regulation of tPA activity was observed. tPA also participates in various forms of chronic neurodegeneration. Accordingly, we assessed tPA activity levels in mouse models of Alzheimer's disease (AD) and spinocerebellar ataxia type-1 (SCA1). Decreased tPA activity was detected in the cortex and subcortex of AD mice, whereas increased tPA activity was found in the cerebellum of SCA1 mice. These findings extend the existing hypotheses that low tPA activity promotes AD, whereas increased tPA activity contributes to cerebellar degeneration. Collectively, our results exemplify the utility of the amidolytic assay and emphasise tPA as a complex mediator of brain function and dysfunction. On the basis of this evidence, we propose that alterations in tPA activity levels could be used as a biomarker for perturbations in brain homeostasis.

Laboratory Investigation (2011) 91, 1079–1091; doi:10.1038/labinvest.2011.67; published online 25 April 2011

KEYWORDS: alzheimer's disease; amidolytic assay; head trauma; morphine; seizure; spinocerebellar ataxia; stroke; tissue-type plasminogen activator

Tissue-type plasminogen activator (tPA) and urokinase plasminogen activator (uPA) are the two main proteases responsible for cleaving the inactive plasminogen into active plasmin. tPA, although best known as an initiator of intravascular fibrinolysis, is also widely expressed in the central nervous system (CNS) in which it mediates numerous physiological (eg memory, reward and anxiety) and pathological (eg seizure and blood–brain barrier breakdown) processes.^{1–3}

Given these recognised neural roles for tPA, there is need for an efficient and sensitive assay to measure tPA activity in brain tissues. There are several existing methods for the detection of tPA activity, including zymographic, amidolytic, immunocapture/ELISA-based and clot lysis assays. Although all of these assays are optimised and routinely used for the detection of tPA activity in plasma and other bodily fluids,^{4–7} most studies to date have used only zymography to monitor

¹Australian Centre for Blood Diseases, Monash University, Melbourne, VIC, Australia; ²Department of Pharmacology, The University of Melbourne, Parkville, VIC, Australia; ³Florey Neurosciences Institute, University of Melbourne, Parkville, VIC, Australia; ⁴Centre for Neuroscience, University of Melbourne, Parkville, VIC, Australia; ⁵Department of Pathology, University of Melbourne, Parkville, VIC, Australia; ⁶Centre for Neuroscience, University of Melbourne, Parkville, VIC, Australia; ⁷Department of Medicine, Royal Melbourne Hospital, University of Melbourne, Parkville, VIC, Australia and ⁸Department of Genetic Medicine and Development, Faculty of Medicine, University of Geneva, Switzerland

Correspondence: Professor R Medcalf, PhD, Australian Centre for Blood Diseases, Monash University, Level 6, Burnet Building, 89 Commercial Road, Melbourne 3004, VIC, Australia.

E-mail: robert.medcalf@monash.edu

*These authors contributed equally to this work.

Received 27 October 2010; revised 27 February 2011; accepted 1 March 2011

the *in vivo* changes in tPA activity in the brain. In this study, we have used a fibrin-dependent amidolytic assay, used previously in other settings,⁸ to rapidly quantitate changes in net tPA proteolytic activity in mouse brain tissues. The optimised amidolytic assay described in this study is preferentially suited to specifically quantitate tPA activity in mouse brain extracts.

By using this assay, we have quantified fluctuations in tPA activity during mouse models of opiate administration, electrically evoked (kindled) seizures, traumatic brain injury (TBI) and ischaemic stroke. Each of these conditions has been linked with changes in endogenous tPA expression. Following morphine administration, tPA activity levels were significantly increased in the cortex, but were reduced in the cerebellum. In contrast, seizure induction triggered a significant and global increase in tPA activity in all tested neural compartments. tPA activity levels were also altered in acute CNS injury paradigms. Cortical tPA activity was increased within the lesion following TBI, but unexpectedly decreased following an ischaemic stroke. Neither stroke nor TBI altered tPA activity levels in the cerebellum.

Further, we used the amidolytic assay to quantify changes in tPA activity in two models of chronic neurodegeneration: the APP^{swe}/PS1^{dE9} mouse model of Alzheimer's disease (AD) and the 154Q/2Q knock-in mouse model of spinocerebellar ataxia type-1 (SCA1). Strengthening the association between suppressed tPA activity and increased amyloid burden, we found that tPA activity was decreased in the cortex and subcortex of young APP^{swe}/PS1^{dE9} mice. Interestingly, opposite trends arise during cerebellar degeneration, with increased tPA activity present in the cerebella of mice that express a pathogenic form of Ataxin-1—the mutant protein responsible for SCA1. Increased tPA activity observed in three genetically distinct models of cerebellar degeneration^{9,10} suggests that high levels of tPA may causally contribute to cerebellar degeneration.

Although this study did not investigate the physiological or pathological consequences of these changes in tPA expression, that subtle and tight regulation of tPA activity occurred across such a wide variety of neurological situations highlights the complex and important neuromodulatory role of tPA in the CNS.

MATERIALS AND METHODS

Materials

S2251 was from Chromogenix AB (Mölnådal, Sweden). Human plasminogen and plasminogen-depleted human fibrinogen were from Calbiochem (Merck, Victoria, Australia). Cyanogen bromide-digested fibrinogen (CNBr-fibrinogen) was from American Diagnostica (Stamford, CT, USA). Skim milk powder was from Diploma (Bonlac Foods, Melbourne, Australia). Morphine hydrochloride was from Glaxo Australia (Boronia, Australia).

Animals

All animal procedures were undertaken in accordance with the National Health and Medical Research Council Code of Practice for the Care and Use of Animals for Experimental Purposes in Australia. Experiments were performed with adult male mice on the C57/Bl6-J background aged 8–12 weeks (except for APP^{swe}/PS1^{dE9} mice; see below), and approved by the appropriate Institutional Animal Ethics Committees. T4 mice are transgenic mice that constitutively produce increased levels of tPA in post-natal neurons.¹¹ tPA^{-/-} mice¹² were obtained from a homozygote breeding line and backcrossed 13 generations. SCA1 and wild-type (WT) littermate mice¹³ were obtained from a heterozygote breeding colony. APP^{swe}/PS1^{dE9} mice were obtained from Jackson Laboratory (#004462; Bar Harbor, ME, USA and bred at the Department of Pathology at the University of Melbourne; amyloid precursor protein (APP) gene containing the Swedish mutation and the presenilin (PS1) gene containing a deleted exon-9). These mice express the chimeric mouse/human variant.¹⁴

Extraction of Tissue from Naive Mice

Wild-type, tPA^{-/-} and T4 transgenic mice were transcardially perfused with 30 ml phosphate-buffered saline (PBS), pH 7.4. Brains were removed and 2-mm coronal sections were prepared using a Mouse Brain Blocker (Kopf, Germany). The hippocampus, striatum, cortex and cerebellum were then dissected from these sections. Each compartment was weighed and homogenised to a final concentration of 150 mg of tissue/ml in PBS + 1% Triton X-100.

Morphine Treatment

Wild-type mice were given a single intraperitoneal injection of morphine hydrochloride (dissolved in sterile 0.9% saline) at a dose of 20 mg/kg. Control mice were injected with the same volume of a sterile 0.9% saline solution. At 2-h post-administration, mice were anaesthetised with an intraperitoneal injection of 25% (w/v) urethane (3.3 g/kg), and then transcardially perfused with 30 ml of PBS, pH 7.4. The cortex, sub-cortical regions and cerebellum were then dissected out, weighed and homogenised to a final concentration of 150 mg/ml in PBS containing 1% Triton X-100.

Real-Time PCR Quantitative mRNA Analysis

RNA was extracted from PBS-perfused brain tissue using the RNeasy Lipid Tissue kit (Qiagen, Germany). Complementary DNA was synthesised using 1 µg of RNA through a reverse transcription reaction (Superscript II, Invitrogen, USA). tPA transcript levels were determined by one-step qRT-polymerase chain reaction (PCR) assays using Brilliant II SYBR green qRT-PCR master mix (Stratagene) in a Mastercycler ep gradient S (Eppendorf, Germany) using the SYBR-green fluorescence quantification system (Biotools, Spain). The reactions were incubated in a 96-well optical plate at 95°C for 10 min, followed by 40 cycles of 95°C for 15 s and 60°C for 10 min. The threshold cycle (Ct) is defined as the fractional

cycle number at which the fluorescence passes the fixed threshold.

The primer sequences used were APRT Forward: 5'-GATCCTTCCGAGCTTCCATCC-3' and APRT Reverse: 5'-CC TGGAGTCTAGACCTGCGATG-3'; tPA Forward: 5'-TGGC TCCGACCCATGCTCAGAA-3' and tPA Reverse: 5'-TCGCT GCAACTTCGGACAGGCA-3'.

Amygdala-Kindling Seizure Model

Surgical procedure

Bipolar stimulating electrode implantation surgery was performed as previously described,¹⁵ and modified for mice. Briefly, animals were anaesthetised by injection of a cocktail of ketamine (100 mg/kg) and xylazine (20 mg/kg), and positioned in a stereotaxic frame. A midline incision was made along the scalp, and three holes were drilled into the skull. Gold 'male' connector electrodes (Farnell In One, Chester Hill, Australia) previously soldered onto nickel alloy jeweller's screws were then screwed into the holes to serve as electroencephalogram (EEG) recording electrodes. Using stereotaxic guidance, a fourth hole was drilled into the skull, and a bipolar electrode (Plastics One, Roanoke, VA, USA) was inserted into the left basolateral amygdala complex (AP: -1.5 mm; ML: -3.5 mm relative to bregma; DV: -4 mm relative to the dura). Dental cement was applied to the skull to keep electrodes in place, and the skin then sutured around the headpiece. Mice were allowed to recover from surgery for at least 7 days before commencement of electrical kindling.

Electrical amygdala kindling

Following recovery, each mouse was randomised to receive electrical kindling stimulations or sham stimulations. For kindled mice, electrical stimulations were applied via the bipolar electrode using an Accupulser Pulse Generator/Stimulator (A310, World Precision Instruments, Sarasota, FL, USA) connected to a battery-operated, optically isolated, constant stimulus isolator (A360, World Precision Instruments). Stimulations were administered twice daily with at least 4 h in between stimulations. The stimulations consisted of a 1-s train of 1-ms biphasic square wave pulses at a frequency of 60 Hz with current intensity of 200 μ A. Sham-kindled animals were gently handled, and the stimulating cable attached to the head piece for 3 min twice daily. Electrical stimulation, resulting in behavioural seizures were measured on the EEG and scored behaviourally using the Racine scale.¹⁶ Kindling persisted until each animal reached the 'fully kindled state' (ie five class V seizures). Once at this point, each kindled mouse was left undisturbed for 7 days. This delay was considered crucial to separate the acute short-term effects of a seizure from the effects of seizures experienced in the preceding days.

Tissue harvest

At 1 week after kindled mice reached the fully kindled state, each animal received a final electrical stimulation (or sham

stimulation), and the seizure recorded on EEG and graded for behavioural class. At 4 h following this stimulation, animals were killed by lethal injection of pentobarb (63 mg/kg) and cardiac-perfused with PBS. The brains were then excised and the contralateral hippocampus, motor cortex and amygdala/piriform cortex regions dissected under a microscope, and processed as above.

Mouse Focal Cerebral Ischaemia Model

Wildtype mice were subjected to transient cerebral ischaemia induced by 2 h middle cerebral artery occlusion (MCAo) followed by 30 min reperfusion as previously described.¹⁷ Mice were anaesthetised with urethane (3.3 g/kg), transcardially perfused with PBS, and the brain tissues dissected and homogenised as described above.

Controlled Cortical Impact (CCI) Model of Traumatic Brain Injury

The electromagnetic CCI device was assembled as described.¹⁸ Following anaesthesia with 2,2 tribromoethanol (0.5 mg/kg) WT mice were placed in a stereotaxic frame (Kopf, Tujunga, CA). A surgical incision was made, the skull was exposed and a 3-mm diameter circular craniotomy was performed with a burr drill over the left parietal cortex, with the centre at coordinates AP = -2.0, ML = +2.0 from bregma. The impactor was positioned at an angle of 20° to the dural surface and adjusted until the tip was centred within the craniotomy. The impactor tip was slowly lowered until the tip just contacted the dura. The cortical impact was initiated through the graphical user interface of the software that controlled the CCI device. First, there was a retraction of the tip of 30 mm, and then a downward strike of 31 mm (velocity: 5 m/s; dwell time 150 ms), resulting in a mild to moderate TBI at an impact depth of 1 mm. The exposed site was then covered with bone wax, the scalp was sutured and the animals were allowed to recover on a 37°C heat pad. At 3 h post-trauma, mice were anaesthetised with urethane (3.3 g/kg), transcardially perfused with PBS, and the brain tissues dissected and homogenised as described above.

In all experimental paradigms, homogenisation of 150 mg brain tissue per ml PBS-Triton X-100 consistently produced lysates of 0.25 mg of protein per ml as determined by ThermoFisher Scientific BCA assay (data not shown).

Alzheimer's Disease (APPswe/PS1dE9) Mice

APPswe/PS1dE9 mice (4-week-old male) and their littermate controls were anaesthetised with urethane (3.3 g/kg), and brain tissues dissected and homogenised as described above. Note, because of animal procedure restrictions, the APPswe/PS1dE9 mice and their littermate controls were not transcardially perfused with PBS before tissue collection.

Spinocerebellar Ataxia Type-1 Mice

Male SCA-1 mice and their littermate controls were killed by CO₂ inhalation, and the brain tissues dissected and

homogenised as described above. Note, because of animal procedure restrictions, the SCA1 mice and their littermate controls were not transcardially perfused with PBS before collecting tissues.

Amidolytic Assay for Mouse Brain-derived tPA

This method was based on the amidolytic assay initially described by,⁸ with modifications for the optimal detection of tPA in mouse brain extracts. Mouse brain lysates were centrifuged at 13 000 *g* for 2 min at 4°C to pellet cellular debris (use of lysates with no previous centrifugation provided data with identical trends but greater variance; data not shown). A volume of 20 μ l of supernatant was transferred to an ice-cooled 96-well plate to which S2251 and CNBr-fibrinogen were added to final concentrations of 2 mM and 0.1 mg/ml, respectively. Plasminogen was then added to a final concentration of 0.5 μ M and the reactions were made up to a final volume of 70 μ l in PBS. Mineral oil was then placed on the top of every well. Absorbance at $\lambda = 405$ nm was measured every 2 min for 6–8 h at 37°C using a fluorescence plate reader (BMG Fluostar Optima). As previously described,¹⁹ second-order polynomial equations were best-fitted to each 'absorbance at $\lambda = 405$ nm vs time' curve using GraphPad Prism Version 4.03 software. The second-order coefficient of each best-fit polynomial equation was taken as half the initial rate of the amidolytic assay.

Polyacrylamide Gel Electrophoresis (PAGE)-based Fibrin Zymography

Sodium dodecyl sulphate (SDS)-PAGE-based fibrin zymography was performed as described.⁴ In brief, 10 μ l of mouse brain lysates (at 150 mg of tissue/ml) were subjected to non-reduced SDS-PAGE. After electrophoresis, gels were washed in 2.5% Triton X-100 for 1.5 h, then placed on top of a fibrin/agarose:plasminogen matrix and incubated in a humidified 37°C oven until lytic zones were evident. Images were captured at various incubation times using a flatbed document scanner.

Well-based Fibrin Zymography

Five microlitres of mouse brain lysates (at 150 mg of tissue/ml) were added directly to wells (~4 mm diameter) punched from a fibrin/agarose:plasminogen matrix prepared as described above. Gels were then incubated in a humidified 37°C oven until lytic zones were evident. Images were captured at various incubation times using a flatbed document scanner.

In situ Zymography

In situ zymography was performed as described.²⁰ In brief, mice were anaesthetised with urethane (3.3 g/kg), transcardially perfused with ice-cold PBS, following which their brains removed, frozen, and 20 or 40 μ m sections prepared using a cryostat. The overlay mixture (10 mM Tris-HCl, pH 7.4, 1% (w/v) low-melt agarose, 4% boiled skim milk, 0.1% Triton X-100 and 12.5 μ g/ml plasminogen) was prepared at 50°C and 400 μ l was applied evenly onto pre-warmed brain sections on glass slides and glass coverslips added. The slides were incubated for 4–12 h in a humidified 37°C oven until lytic zones were evident. Images were captured under dark-field illumination using an upright Olympus BX50 light microscope (PlanAPO air objective, $\times 1.25$ magnification, numerical aperture 0.04) equipped with a digital camera.

Immunoblotting

Samples were boiled in SDS-loading buffer with dithiothreitol, subjected to SDS-PAGE and transferred onto polyvinylidene fluoride membranes. Membranes were probed with primary antibodies (sheep anti-mouse neuroserpin (gift from Prof Daniel A Lawrence; Ann Arbor, MI, USA); rabbit anti-mouse PAI-1 (gift from Prof Daniel A Lawrence); '4B3' mouse anti-rat PN-1 (gift from Prof Denis Monard; Basel, Switzerland); W02 mouse anti-human β 1-16²¹ to detect APP, mouse tubulin (Sigma T0198) and mouse anti-GAPDH (Millipore MAB374) followed by the appropriate HRP-conjugated secondary antibody. Signals were revealed by chemiluminescence (ThermoScientific).

Statistical Analyses

The Student's *t*-test was used to compare rates of plasminogen activation in Figures 1-4, 5a, 6 and 7. One-way ANOVA with Newman-Keul's *post-hoc* analysis was used to compare rates of plasminogen activation in Figure 5c and Supplementary Figure S2.

RESULTS

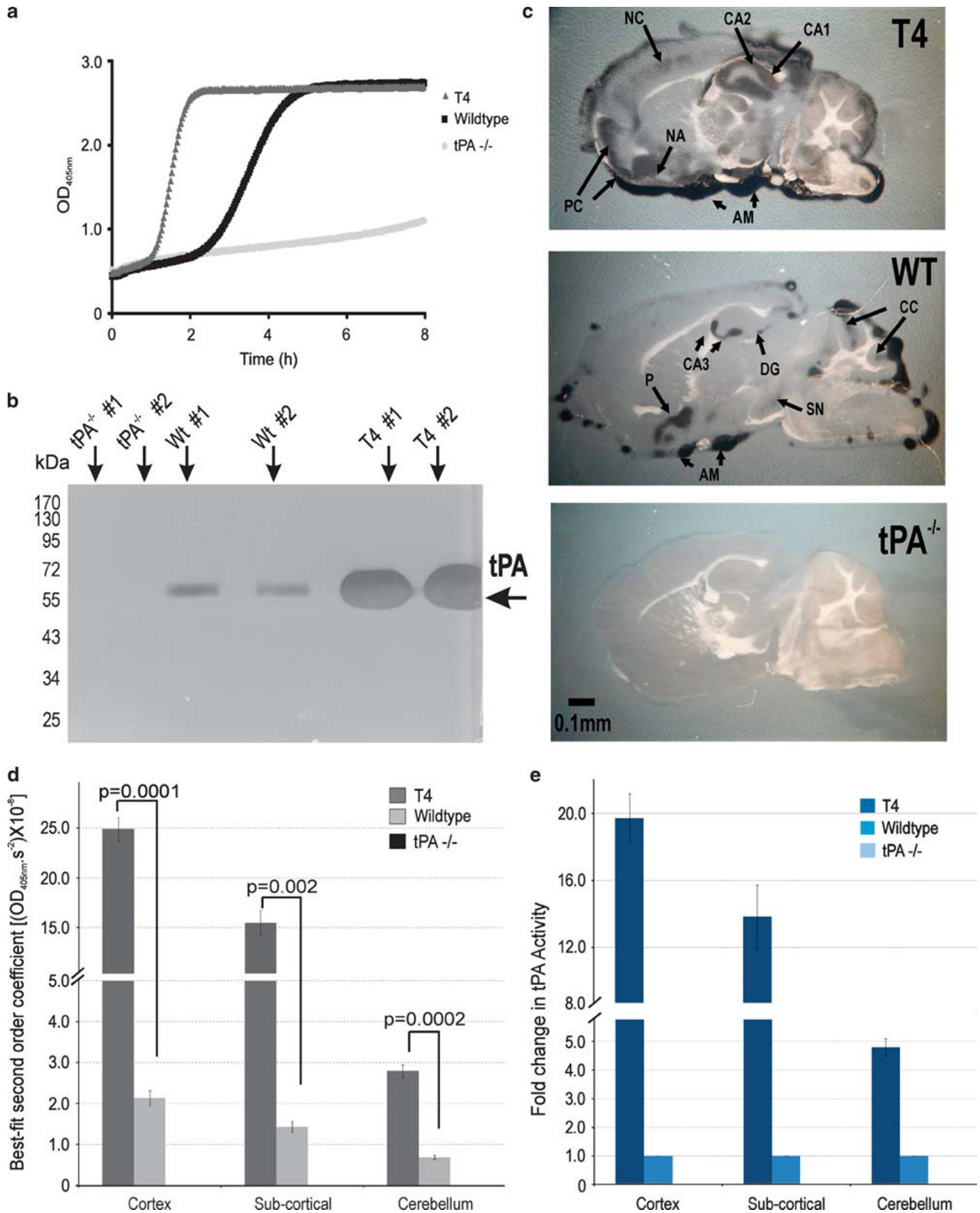
Amidolytic Assay

Our main objective was to harness a previously described amidolytic assay⁸ to enable the accurate determination of net tPA activity in mouse brain extracts. Accordingly, we quantified tPA-mediated plasminogen activation in brain tissue extracted from WT, T4 transgenic mice and tPA^{-/-} mice to determine the reliability, sensitivity and reproducibility of the amidolytic assay. In these experiments, we have expressed the

Figure 1 Comparison of the amidolytic assay and zymographic techniques using tissue-type plasminogen activator (tPA)^{-/-}, wild-type (WT) and T4 mice. (a) Raw data of an amidolytic assay using cortical lysates from a T4, WT and tPA^{-/-} mouse. (b) PAGE-based fibrin zymography of cortical lysates from two T4, two WT and two tPA^{-/-} mice. (c) *In situ* zymography of sagittal brain sections from a T4, WT and tPA^{-/-} mouse. Photographs were taken after 9 h incubation at 37°C. To ensure a comparable degree of lysis, 40 μ m section of tPA^{-/-} and WT mouse brains and 20 μ m sections of the T4 mouse brain were used. Abbreviations: P, pallidum, AM, amygdala, CA1-3, cornu ammonis 1-3, DG, dentate gyrus, SN, substantia nigra, CC, cerebellar cortex, PC, piriform cortex, NA, nucleus accumbens and NC, Neocortex. (d) Nonlinear regression analyses from the amidolytic assays have been expressed as 'best-fit second-order coefficients' (amidolytic assay rate) and were performed on lysates of the cortex, sub-cortical regions and cerebellum of T4, WT and tPA^{-/-} mice. (e) Fold-change in tPA activity in T4 and tPA^{-/-} relative to WT cortex, sub-cortical regions and cerebellum (*n* = 3 per genotype; data represents mean \pm s.e.m.). Data derived from panel d.

rate of change in S2251 hydrolysis (as determined by changes in OD_{405 nm}) in the presence of CNBr-fibrinogen over time as the 'best-fit second-order coefficient'. As shown in Figure 1a,

the change in OD_{405 nm} followed a sigmoidal curve. To derive the amidolytic assay rates from these curves, the first ~20 min of the reaction and all values above the inflexion



point were excluded as this was found to result in a line of best-fit that better approximated the raw data. A second-order polynomial equation (ie $a + bx + cx^2 = y$) was best-fitted to the remaining data using nonlinear regression analysis, in which the second-degree coefficient 'c' equates to half the rate of the amidolytic assay. The absence of plasminogen activation in the samples from tPA^{-/-} mice demonstrates that tPA is the predominant plasminogen activator present in these brain lysates (Figure 1a). SDS-PAGE-based fibrin zymography of cortical lysates from T4, WT and tPA^{-/-} mice (Figure 1b) also confirmed that tPA is the main plasminogen activator in the mouse brain as urokinase (urokinase plasminogen activator; ~47 kD) was not detected upon incubation times shorter than 24 h. Figure 1a also shows that changes in the rate of the amidolytic assay correspond to changes in tPA levels in mouse brain lysates. By applying this amidolytic assay to quantitate tPA activity in a 1:2 dilution series of cortical extracts obtained from a T4 mouse, we were able to determine a relationship between relative tPA activity and the rate of the amidolytic assay (Supplementary Figure S1). This relationship followed a two-phase exponential curve with the equation $y = 546.5(1 - 10^{(-181612 \cdot x)}) - 11.13(1 - 10^{(-6700000 \cdot x)})$, where x is the rate of plasminogen activation and y is the dilution factor (in %) of the T4 cortical lysate (Supplementary Figure S1). A ratio of the calculated y values provides a fold-change in tPA activity. For example, Figure 1d shows the best-fit second-order coefficient, or rate of the amidolytic assay and Figure 1e shows fold-changes in tPA activity that were derived from Figure 1d. In all subsequent figures, both the 'best-fit second-order coefficient' and the derived 'fold-change in tPA activity' are presented in different panels.

Quantitation of the amidolytic assay shows tPA activity in the T4 mice was increased by a factor of 17.7, 11.8 and 4.8 in the cortex, sub-cortical structures and cerebellum, respectively, compared with litter-matched WT mice (Figure 1e). The compartmental differences in tPA overexpression in the T4 mice most likely reflects the relative potency of the Thy1.2 promoter, which drives strong expression in the hippocampus and cortex and weaker expression in the cerebellum (using Allen's on-line brain atlas software v.1.4.2; not shown).

We were also able to use the amidolytic assay to assess net tPA activity in various brain compartments in naive WT C57Bl6 mice, and found that tPA activity is the highest in the cortex (relative to the hippocampus, striatum and cerebellum; Supplementary Figure S2). We next performed *in situ* zymography on sagittal brain sections from T4, WT and tPA^{-/-} mice (Figure 1c). As expected, high tPA activity levels were evident in the cerebellar cortex, the hippocampus (CA3 and dentate gyrus), the amygdala and the pallidum (Figure 1c), with lower activity evident in the substantia nigra of WT mice. Prominent tPA activity was also observed in the pial vessels and meningeal membranes. tPA activity levels were significantly elevated in all neural structures in T4 mice, most notably in the CA1 and CA2 regions of the hippocampus, the

amygdala, the nucleus accumbens and the piriform areas of the cerebral cortex (Figure 1c). *In situ* zymography on the tPA^{-/-} mouse brain revealed no zones of lysis (Figure 1c), again emphasising that tPA is the predominant plasminogen activator of the murine CNS.

When comparing the amidolytic assay with SDS-PAGE- and *in situ* zymography, it was apparent that each assay was capable of detecting tPA in the mouse brain, however, the amidolytic assay was more sensitive and showed markedly better resolution (compare Figure 1e with Supplementary Figure S3). For instance, whereas the amidolytic assay detected a ~18-fold difference in tPA activity between the cortex of T4 and WT mice, SDS-PAGE-based fibrin zymography detected a ~threefold difference and well-based fibrin zymography only a ~twofold difference (compare Figure 1e with Supplementary Figure S3).

As exemplified in Supplementary Figure S1, we were able to detect tPA activity even when T4 cortical lysates were diluted to 0.05% of their original protein concentration, which was below the detection limit of the zymographic assays under the conditions used (data not shown). Moreover, the high throughput and quantitative nature of the amidolytic assay renders it as an attractive method for detecting tPA levels in the brain.

To demonstrate the utility of the amidolytic assay, we measured changes in tPA activity across numerous neurological situations in which tPA-mediated proteolysis has a functional bearing: opiate administration (Figure 2), electrically evoked seizure (Figure 3), experimental stroke (Figure 4), neurotrauma (Figure 5), AD (Figure 6) and cerebellar degeneration (Figure 7).

Changes in Brain-derived tPA Activity *In vivo* Following CNS Stimulation

Administration of morphine for 2 h caused tPA activity to increase by 10% in the cortex and 23% in the underlying sub-cortical structures (Figure 2). Our findings are consistent with those of Nagai *et al*²² who used SDS-PAGE-based zymography to show that subcutaneous administration of morphine increased tPA activity in numerous compartments of the mouse brain at a similar time point.²² Interestingly, we observed that the single injection of morphine caused tPA activity in the cerebellum to decrease by approximately 27% compared with saline-treated controls (Figure 2). Using real-time PCR reaction, we also demonstrated that tPA mRNA levels followed a similar trend and were marginally higher in the cortex, significantly increased in the sub-cortical structures ($P < 0.05$) and lower in the cerebellum (Supplementary Figure S4). Hence, morphine-induced changes in tPA activity were largely mirrored by changes in tPA mRNA abundance, suggesting a direct effect of morphine on tPA gene expression.

As another model of acute CNS stimulation, we induced seizures in WT mice using the amygdala-kindling model (Figure 3). tPA has been shown to be upregulated following seizure in rats²³ and also implicated in seizure propagation.²⁴

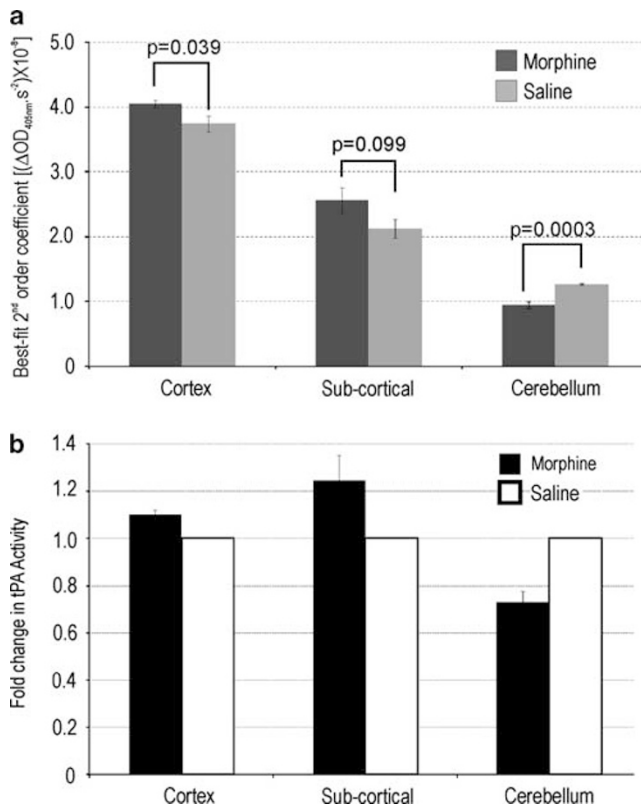


Figure 2 Changes in net tissue-type plasminogen activator (tPA) activity following morphine administration. (a) Nonlinear regression best-fit second-order coefficients from amidolytic assays were performed on lysates of the cortex, sub-cortical regions and cerebellum of wildtype (WT) mice at 2 h after intraperitoneal administration of saline or morphine. (b) Fold-change in tPA activity in morphine vs saline administered groups ($n=5$ per treatment group; data represents mean \pm s.e.m.). Data derived from panel a.

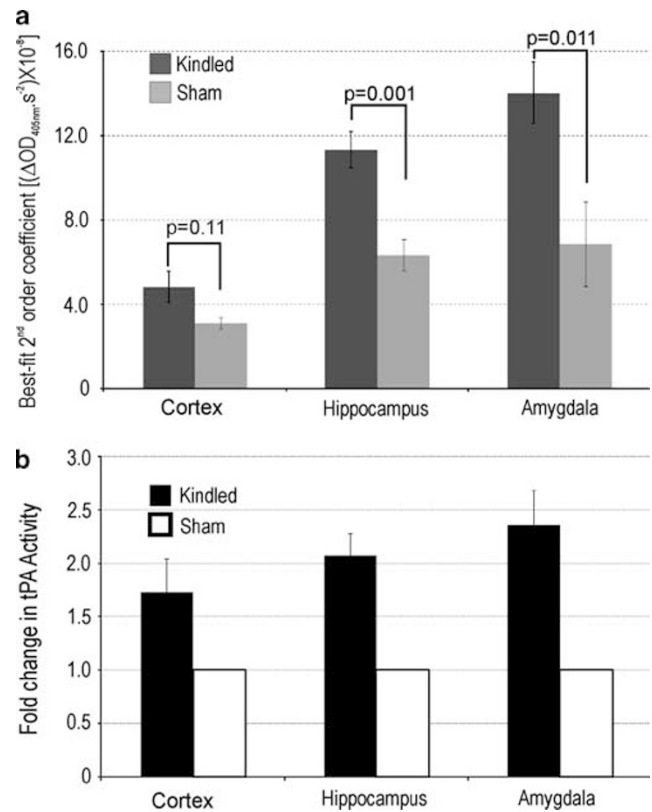


Figure 3 Changes in net tissue-type plasminogen activator (tPA) activity following amygdala kindled-seizures. (a) Nonlinear regression best-fit second-order coefficients from amidolytic assays were performed on lysates of the cortex, hippocampus and amygdala of wild-type (WT) mice at 4 h post-seizure. (b) Fold-change in tPA activity in stimulated vs sham groups ($n=11$ kindled and $n=6$ sham; data represents mean \pm s.e.m.). Data derived from panel a.

For our seizure experiments, the final electrical stimulation induced convulsive seizures with secondary generalisation in all mice (class IV/V), and lasted an average of 36.9 ± 4 s (mean \pm s.e.m.), as measured by review of EEG. At 4 h after this seizure, the amidolytic assay showed a 73, 107 and 135% increase in the motor cortex, hippocampus and amygdala/piriform cortex, respectively, (Figure 3). Notably, unlike the other scenarios used in this study, seizure induction caused a global, rather than a compartment-specific increase in tPA activity.

Changes in Endogenous Brain-derived tPA Activity Following Acute CNS Injury

We next analysed tPA activity levels in mice that had been subjected to transient focal cerebral ischaemia, whereby unilateral ischaemia was induced by MCAo for 2 h followed by a 30 min period of reperfusion. As shown in Figure 4, compared with the uninjured contralateral cortex, a 27.5% reduction in net tPA activity was observed in the ipsilateral cortex. The same trend was observed in the sub-cortical structures (a nonsignificant 15% reduction), whereas tPA

activity was unaltered in the cerebellum following MCAo (Figure 4).

We also assessed changes in tPA activity using the controlled cortical impact model of TBI as another form of acute cerebral injury. Interestingly, at 1 and 3 h after TBI in WT mice, tPA activity levels in the ipsilateral cortex increased by 28–29% relative to the contralateral cortex, but returned to control levels by 24 h after injury (Figures 5c and d). No increases in tPA activity were observed in the ipsilateral cortex of sham-operated animals (Figures 5c and d). As expected, no increases in tPA were observed in the sub-cortical structures or cerebellum following trauma (Figures 5a and b).

Alteration in Endogenous Brain-derived tPA Activity in Chronic Neurodegenerative Diseases

Having assessed several acute models of CNS injury, we next wanted to quantitate tPA activity levels in a chronic neurodegenerative model of AD. Accordingly, we obtained brain tissue homogenates from 4-week-old APP^{Swe}/PS1^{dE9} male mice and litter- and age-matched WT mice.¹⁴ The amidolytic assay revealed a 15 and 26% decrease in tPA activity in the

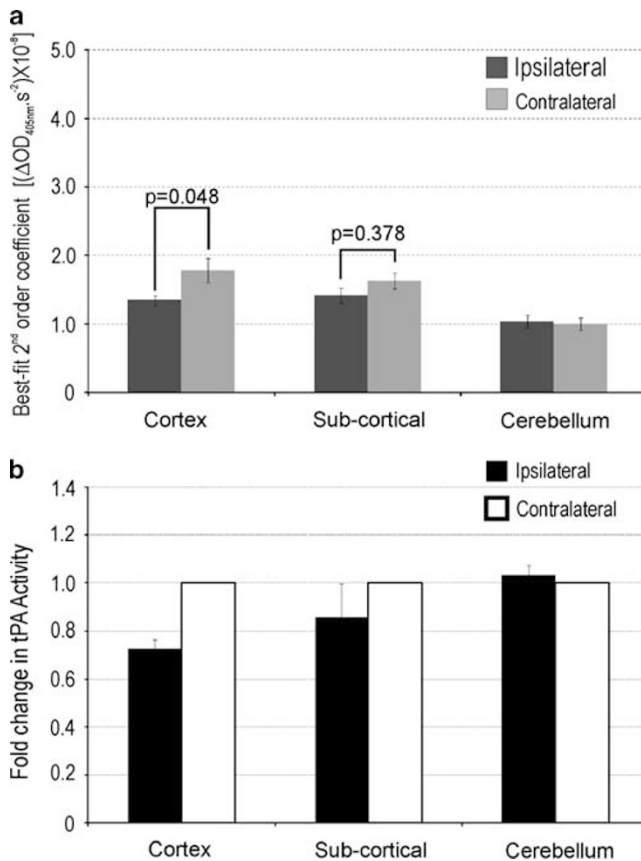


Figure 4 Changes in net tPA activity following middle cerebral artery occlusion (MCAo) and reperfusion. **(a)** Nonlinear regression best-fit second-order coefficients from amidolytic assays were performed on lysates of the cortex, sub-cortical regions and cerebellum of wild-type (WT) mice after 2 h of MCAo and 30 min reperfusion. **(b)** Fold-change in tPA activity in ipsilateral vs contralateral groups ($n=5$ per treatment group; data represents mean \pm s.e.m.). Data derived from panel **a**.

cortex and sub-cortex of APP^{swe}/PS1^{de9} mice (Figure 6). No significant difference in tPA activity was detected in the cerebellum of APP^{swe}/PS1^{de9} mice, a compartment unaffected in APP^{swe}/PS1^{de9} mice. tPA activity levels are known to be influenced by endogenous serine protease inhibitors in the brain, including plasminogen activator inhibitor-1 (PAI-1), protease nexin-1 (PN-1) and neuroserpin. However, we saw no change in cortical levels of PAI-1, PN-1 or neuroserpin in APP^{swe}/PS1^{de9} mice (Figure 6c) at 4 weeks of age. As hypothesised by Liu *et al*,²⁵ elevated β -amyloid load may directly downregulate tPA levels.

Finally assessment of net tPA activity in brain tissue homogenates obtained from 8- to 9-week-old SCA1 mice and litter- and age-matched WT mice revealed a 34% increase in cortical tPA activity levels in SCA1 mice (Figure 7). Although tPA activity levels in the sub-cortical structures were unaffected by SCA1, cerebellar net tPA activity was increased by 23% in the SCA1 mice (Figure 7). In line with our results, a microarray showed elevated tPA mRNA levels in the cerebellum of SCA1 mice at 4 and 12 weeks of age (GEO accession # GDS1756). Importantly, the elevation in

cerebellar net tPA activity in SCA1 mice coincides with reduced motor function as determined by rotarod analysis.¹³

DISCUSSION

There are several well-established methods for the detection of endogenous tPA activity. To date, the vast majority of researchers have used zymography to detect *in vivo* changes in tPA activity in brain tissues; although others have used S2251 amidolytic assays to measure *in vivo* changes in tPA activity.^{9,26–28} In this study we show that this amidolytic assay, long-used as a sensitive and specific means to detect tPA in biological fluids such as plasma,^{6,8} is also useful for determining *in vivo* changes in net tPA activity in mouse brain tissue when tested in the presence of its cofactor, fibrin.

The amidolytic assay offers numerous advantages over zymography. For instance, whereas zymographic methods are semi-quantitative, the amidolytic assay is fully quantitative over a 250-fold dilution range (Supplementary Figure S1). In addition, the resolution of the amidolytic assay is far superior to that of zymographic techniques (compare Figure 1 with Supplementary Figure S3). The amidolytic assay is also exquisitely sensitive and can detect low attomole amounts of tPA (data not shown). Furthermore, the assay is rapid and can be completed within 6 h. The multiwell plate format of the amidolytic assay also offers considerably higher throughput than zymographic procedures.

Mouse brain tissue is well-suited for the amidolytic assay as tPA is far more abundant in the brain than urokinase plasminogen activator.²⁹ Furthermore, the presence of CNBr-fibrinogen accelerates tPA-mediated plasminogen activation more significantly than urokinase plasminogen activator-mediated plasminogen activation.³⁰ The amidolytic assay, although lacking the ability to resolve activity in fine tissue locales, can provide information on net tPA activity within specific dissectible neural compartments in mice, and shows that tPA activity is significantly higher in the cortex when compared with the underlying sub-cortical structures and the cerebellum (Supplementary Figure S2).

One important aspect of the described amidolytic assay is that the relationship between tPA activity and the rate of the amidolytic assay is not linear, but rather follows a two-phase exponential association (Supplementary Figure S1). Because of this nonlinear association, the amidolytic assay should not be used as an end-point assay. Instead, we have used the equation: $y = 546.5(1 - 10^{(-181612 \cdot x)}) - 11.13(1 - 10^{(-6700000 \cdot x)})$ (where x = rate of plasminogen activation and y = dilution in %) to convert experimentally derived changes in the 'rate of the amidolytic assay' into approximate 'fold-change in tPA activity'.

In keeping with tPA having a variety of neuromodulatory roles, our studies clearly show that tPA activity in the CNS is regulated in a compartment-specific and context-dependent manner. For example, systemic morphine administration elicited a 10% increase in cortical tPA activity levels and a 27% decrease in cerebellar tPA activity levels (Figure 2). The

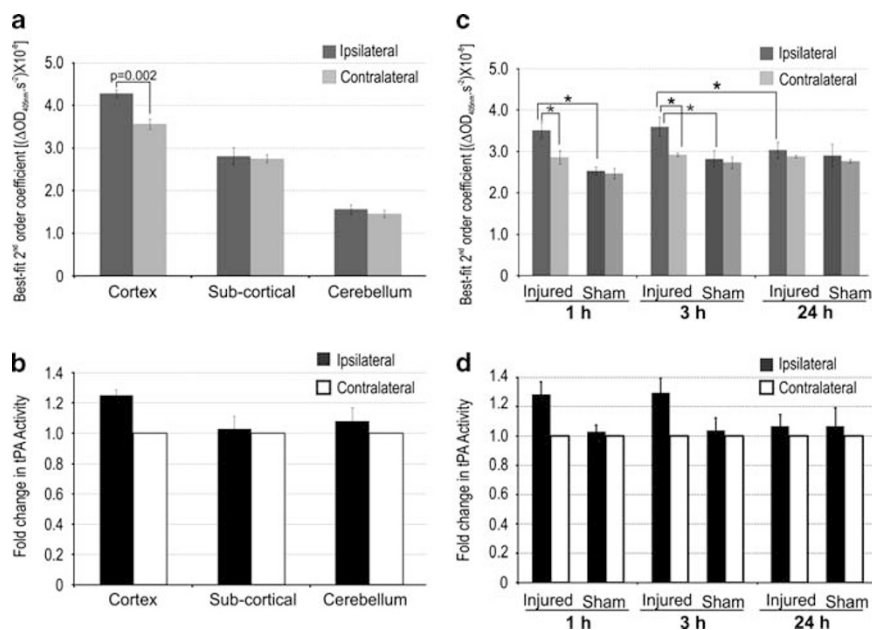


Figure 5 Changes in net tPA activity following traumatic brain injury (TBI). (a) Nonlinear regression best-fit second-order coefficients from amidolytic assays were performed on lysates of the cortex, sub-cortical regions and cerebellum of wild-type (WT) mice 3 h after TBI. (b) Fold-change in tPA activity in ipsilateral vs contralateral groups ($n = 5$ per treatment group; data represents mean \pm s.e.m.). (c) Time course of the rates of plasminogen activation in the ipsilateral and contralateral cortical lysates of WT mice 1, 3 and 24 h post-TBI or post-sham operation. Asterisks indicate $P < 0.05$. (d) Fold-change in tPA activity between ipsilateral vs contralateral groups. Data derived from panel c. ($n = 5$ per treatment group; data represents mean \pm s.e.m.).

downregulation of cerebellar tPA activity following morphine administration was unexpected given that morphine has previously been shown to upregulate tPA levels in the nucleus accumbens, striatum and limbic system.²² Furthermore, tPA activity in the nucleus accumbens is involved in the rewarding and locomotor-stimulating effects of morphine.²² Notably, morphine has recently been identified as an endogenous neuromodulator in the mouse cerebellum, in which GABAergic basket cells release morphine onto the μ -opioid receptors of Purkinje neurons.³¹ We hypothesise that intense activation of Purkinje neurons by exogenous morphine results in the sharp suppression of net tPA activity in the cerebellum. How this downregulation of cerebellar tPA activity influences the behavioural effects of morphine abuse is a topic for future studies.

Seizure activity induced by either chemical or electrical stimulation is recognised to upregulate tPA mRNA in hippocampus,²³ and contributes to seizure propagation throughout brain regions via a plasmin-independent pathway.²⁴ Further, tPA has been demonstrated to be upregulated in brain tissue from human epilepsy patients,³² suggesting a possible role in the epileptic disease state. Studies using tPA^{-/-} mice have also demonstrated that tPA contributes to pathological synaptic plasticity associated with epilepsy, including chemoconvulsant-induced pyramidal cell death³³ and mossy fibre sprouting.³⁴ In this study, we show that tPA enzyme activity is upregulated in limbic and cortical areas of the contralateral hemisphere at 4 h following electrically

evoked seizures (Figure 3). Notably, one study documents a decrease in tPA activity at 24 h post-seizure.³⁵ Our study, however, is consistent with the reports that demonstrate increased tPA gene transcription and increased tPA enzyme activity following seizure.

Investigation into the regulation of tPA activity following acute cerebral injuries also provided unanticipated findings. Although the primary cause of TBI and stroke are vastly different, the secondary mechanisms of brain infarction are overlapping. In particular, excitotoxicity, inflammation, free radical damage and blood-brain barrier breakdown are hallmarks of both TBI and stroke. Moreover, endogenous tPA worsens infarction following both TBI and stroke.^{36,37} On the basis of these commonalities, we predicted that endogenous tPA activity would be regulated in a similar manner during both stroke and TBI.

However, although cortical net tPA activity increased by 29% following TBI (Figure 5), a 26% decrease in tPA activity was observed following MCAo (Figure 4). We also observed that the increase in tPA activity after TBI was an acute phenomenon, commencing as early as 1 h post-injury and persisting till 3 h, but returning to baseline levels at 24 h post-injury. Our findings extend previous studies that document an increase in tPA antigen in the cerebrospinal fluid of pigs within 60 min after TBI,³⁸ an increase in tPA antigen in brain tissue from human TBI autopsy samples³⁹ and an increase in tPA mRNA in the rodent cortex at 4 h after TBI (GEO accession # GDS2850 and GDS2851;⁴⁰).

For MCAo, previous studies have used semi-quantitative SDS-PAGE-based zymography to assess changes in cerebral tPA activity post-MCAo.^{41–44} For instance, Hamann *et al*⁴¹ found no change in tPA activity in the ischaemic cortex, whereas Yepes *et al*⁴² found that cerebral tPA activity

increased 6 h after MCAo. Our findings match those of Rosenberg *et al*,⁴³ in which fibrin zymography was used to show that ipsilateral tPA activity decreased following MCAo in rats. The mechanism by which tPA activity is reduced in the lesion following MCAo was not explored in this study. The reasons for such diametric regulation of tPA activity in TBI and stroke remains unclear, but again highlights the fact that the neural roles of tPA are complex.

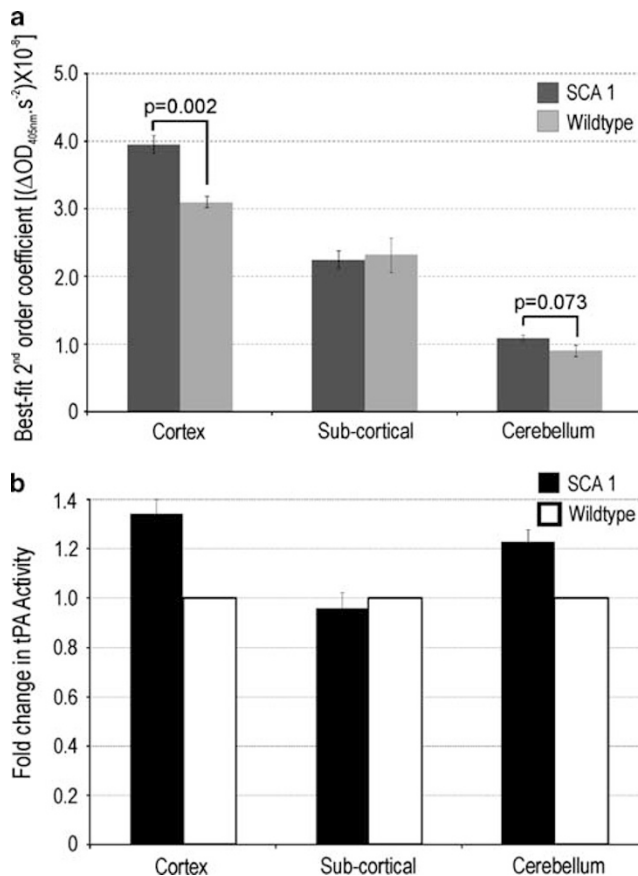
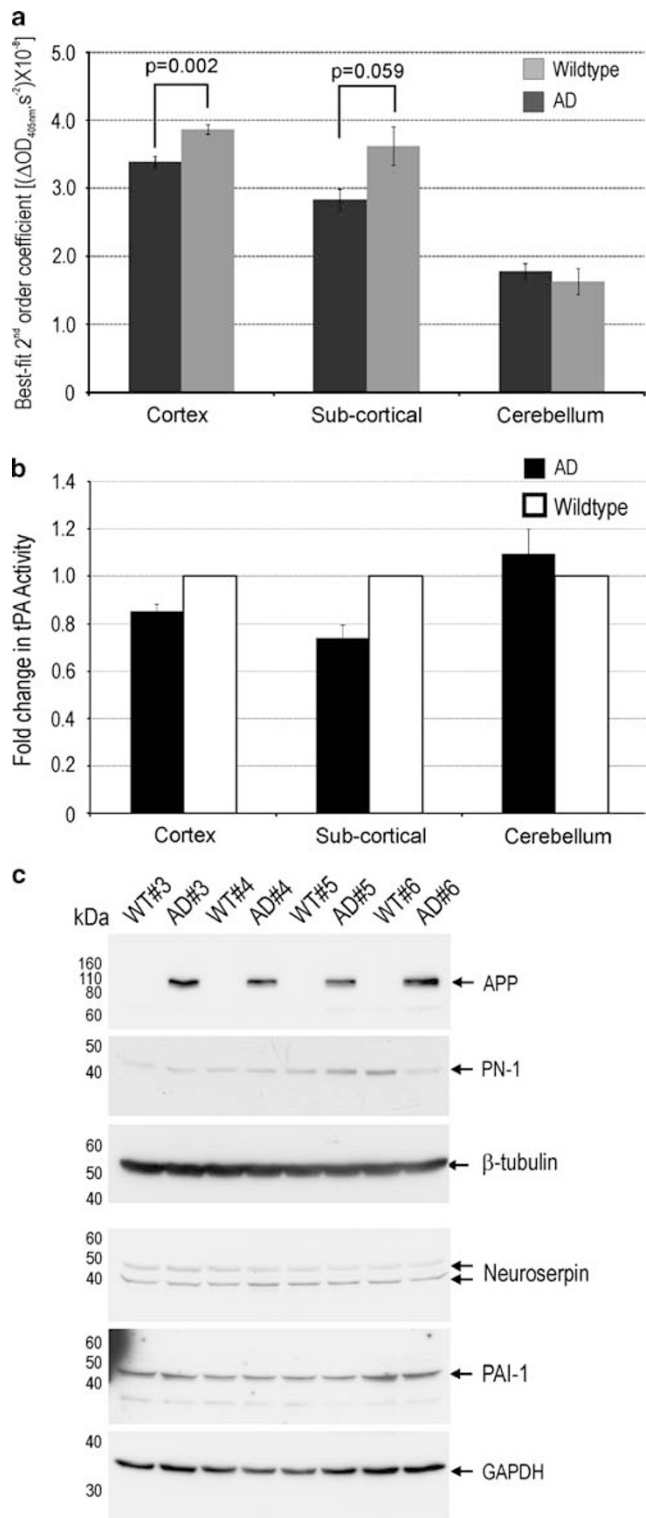


Figure 7 Elevated net tPA activity in spinocerebellar ataxia type-1 (SCA1) mice. **(a)** Nonlinear regression best-fit second-order coefficients from amidolytic assays were performed on lysates of the cortex, sub-cortical regions and cerebellum of transgenic SCA1 mice or their wild-type (WT) littermate controls **(b)** Fold-change in tPA activity in SCA1 vs WT groups ($n = 4$ per genotype; data represents mean \pm s.e.m.). Data derived from panel **a**.

Figure 6 Changes in net tPA activity in a mouse model of Alzheimer's disease. **(a)** Nonlinear regression best-fit second-order coefficients from amidolytic assays were performed on lysates of the cortex, sub-cortical regions and cerebellum of APP/PS1 mice (AD) or their wild-type (WT) littermate controls. **(b)** Fold-change in tissue-type plasminogen activator (tPA) activity in APP/PS1 mice relative to WT groups ($n = 6$ per genotype; data represents mean \pm s.e.m.). Data derived from panel **a**. **(c)** Western blot detection of amyloid precursor protein (APP), plasminogen activator inhibitor-1 (PAI-1), neuroserpin and protease nexin-1 (PN-1) in cortical lysates from APP/PS1 mice (AD) and WT mice. β -Tubulin was used as a loading control for APP and PN-1, and GAPDH was used as a loading control for neuroserpin and PAI-1.

The tPA/plasmin system has long been hypothesised to be a physiological clearance mechanism for β -amyloid.^{45,46} In support of this notion, previous studies that used SDS-PAGE-based zymography have reported decreased cerebral tPA/plasmin activity in brains of human patients with AD.^{47–49} A downregulation of tPA activity is also evident in mouse models of AD, with several studies attributing the suppression of tPA activity to an increase in the expression of serine protease inhibitors.^{25,48,50} Although we also show a decrease in tPA activity in the AD mouse brain, no obvious increases in the expression of the major inhibitors of tPA including PAI-1, PN-1 or neuroserpin was observed (Figure 6c). This dissimilarity may be because of the especially young age of the AD mice used in our study, as increases in PAI-1 levels²⁵ and decreases in tPA expression⁵¹ arise at later stages in development. The suppression of tPA activity in APPswe/PS1dE9 mice at 4 weeks of age (Figure 6) is of particular interest, as plaques and other hallmarks of AD do not appear in these mice until approximately 4 months of age.^{52,53} To our knowledge, this is the earliest stage of development at which suppressed tPA activity has been shown in a mouse model of AD, and further implicates low tPA levels in the progression of AD.

The final situation where we assessed net tPA activity was that of cerebellar degeneration. It has previously been shown that elevated tPA activity precedes cerebellar degeneration in Lurcher mice and Nervous mice—two unrelated models of cerebellar dysfunction.^{9,10} Experimental evidence from both of these models led to the postulate that high levels of tPA activity promote cerebellar degeneration. Accordingly, we measured tPA activity levels in transgenic SCA1 mice. SCA1 is an autosomal dominant form of spinocerebellar degeneration.⁵⁴ The transgenic SCA1 mice used in our study develop many of the neurological and histological signs of the human disorder including ataxia, Purkinje neuron loss and nuclear inclusion formation.¹³ At 8 weeks of age, before the onset of Purkinje neuron loss but coincident with motor dysfunction,¹³ we observed that net tPA activity was 23% higher in the cerebellum of SCA1 mice, relative to their littermate controls (Figure 7). This is the first documentation of cerebellar tPA activity levels being increased in a model of human cerebellar degeneration and supports the theory that elevated tPA activity levels promote cerebellar degeneration. Curiously, increased levels of tPA were also detected in the cortex of SCA1 transgenic mice (Figure 7). The cortex of SCA1 mice displays no significant signs of degeneration, despite prominent SCA1 transgene expression in the cerebral cortical neurons.¹³ These observations raise the possibility that: (1) elevated net tPA activity is not the result of cell injury but is instead likely due to the presence of pathological SCA1 protein, and/or (2) the putative detrimental influence of high tPA activity may be restricted to the cerebellum in SCA1 mice. If high levels of tPA do indeed contribute to cerebellar degeneration, then the T4 transgenic mice would also be expected to display signs of cerebellar stress such as

motor incoordination and Purkinje neuron loss. This hypothesis is currently being tested.

In conclusion, we have harnessed the previously described fibrin-accelerated amidolytic assay to quantify *in vivo* changes in mouse brain-derived tPA activity. Using this amidolytic assay, rapid and differential regulation of tPA activity was observed in mice between the cortex and cerebellum following systemic morphine administration. Rapid, diametric regulation of tPA activity was also observed in the cortex following TBI and stroke. Notably, severe epileptic seizure was the only setting in which a global change in brain tPA activity was observed. Thus, on the basis of the elevated cerebellar tPA activity in SCA1 transgenic mice, we hypothesise that high net tPA activity contributes to cerebellar dysfunction. This study highlights that a tight and context-dependent regulation underlies the complex neurological roles of tPA. On the basis of this exquisite regulation, we also speculate that alterations in neural net tPA activity levels could be used as a biomarker for perturbations in brain stasis.

Supplementary Information accompanies the paper on the Laboratory Investigation website (<http://www.laboratoryinvestigation.org>)

ACKNOWLEDGEMENTS

We thank Prof Norman Saunders, Dr Mark Habgood, Dr Simone Beckham and Mr Adam Galle for constructing the electromagnetic CCI device. We also thank Ms Amanda Au for assisting in the preparation of mouse brain lysates following MCAo. Be'eri Niego for constructive comments regarding the amidolytic assay. Volga Tarlac and Elsdon Storey from the Van Cleef Roet Centre for Nervous Diseases for providing us with the SCA1 mutant and wild-type littermate mice, and Prof John Hamilton (Department of Medicine, Royal Melbourne Hospital) for providing the mice for the seizure studies. This study was supported by grant numbers 606659 awarded to RLM and ALS from the National Health and Medical Research Council (NH&MRC) of Australia and by grant numbers 491152 and 606660 awarded to RLM from the NH&MRC and D0-34 awarded to RLM from the Victorian Neurotrauma Initiative. This study was also supported by grant numbers 628391 and G 08M 3821 awarded to PJC from the NH&MRC and the National Heart Foundation of Australia, respectively, and by grant number 566544 awarded to NCJ from the NH&MRC. AJL and RLM are also supported with Senior Research Fellowships, and NCJ supported with a Career Development Award, from the NH&MRC.

DISCLOSURE/CONFLICT OF INTEREST

The authors declare no conflict of interest.

- Melchor JP, Strickland S. Tissue plasminogen activator in central nervous system physiology and pathology. *Thromb Haemost* 2005; 93:655–660.
- Samson AL, Medcalf RL. Tissue-type plasminogen activator: a multifaceted modulator of neurotransmission and synaptic plasticity. *Neuron* 2006;50:673–678.
- Yepes M, Roussel BD, Ali C, *et al*. Tissue-type plasminogen activator in the ischemic brain: more than a thrombolytic. *Trends Neurosci* 2009;32:48–55.
- Granelli-Piperno A, Reich E. A study of proteases and protease-inhibitor complexes in biological fluids. *J Exp Med* 1978;148:223–234.
- Shimada H, Mori T, Takada A, *et al*. Use of chromogenic substrate S-2251 for determination of plasminogen activator in rat ovaries. *Thromb Haemost* 1981;46:507–510.

6. Eriksson E, Risberg B. Measurement of tissue plasminogen activator in plasma. A comparison of 3 methods and description of a new improved technique. *Thromb Res* 1987;46:213–223.
7. Stephens R, Leung KC, Pollanen J, *et al*. Microplate immunocapture assay for plasminogen activators and their specific inhibitors. *J Immunol Methods* 1987;105:245–251.
8. Verheijen JH, Mullaart E, Chang GT, *et al*. A simple, sensitive spectrophotometric assay for extrinsic (tissue-type) plasminogen activator applicable to measurements in plasma. *Thromb Haemost* 1982;48:266–269.
9. Lu W, Tsirka SE. Partial rescue of neural apoptosis in the Lurcher mutant mouse through elimination of tissue plasminogen activator. *Development* 2002;129:2043–2050.
10. Li J, Ma Y, Teng YD, *et al*. Purkinje neuron degeneration in nervous (nr) mutant mice is mediated by a metabolic pathway involving excess tissue plasminogen activator. *Proc Natl Acad Sci USA* 2006;103:7847–7852.
11. Madani R, Hulo S, Toni N, *et al*. Enhanced hippocampal long-term potentiation and learning by increased neuronal expression of tissue-type plasminogen activator in transgenic mice. *EMBO J* 1999;18:3007–3012.
12. Carmeliet P, Schoonjans L, Kieckens L, *et al*. Physiological consequences of loss of plasminogen activator gene function in mice. *Nature* 1994;368:419–424.
13. Watase K, Weeber EJ, Xu B, *et al*. A long CAG repeat in the mouse Sca1 locus replicates SCA1 features and reveals the impact of protein solubility on selective neurodegeneration. *Neuron* 2002;34:905–919.
14. Jankowsky JL, Slunt HH, Ratovitski T, *et al*. Co-expression of multiple transgenes in mouse CNS: a comparison of strategies. *Biomol Eng* 2001;17:157–165.
15. Salzberg M, Kumar G, Supit L, *et al*. Early postnatal stress confers enduring vulnerability to limbic epileptogenesis. *Epilepsia* 2007;48:2079–2085.
16. Racine RJ. Modification of seizure activity by electrical stimulation. II. Motor seizure. *Electroencephalogr Clin Neurophysiol* 1972;32:281–294.
17. Wong CH, Bozinovski S, Hertzog PJ, *et al*. Absence of glutathione peroxidase-1 exacerbates cerebral ischemia-reperfusion injury by reducing post-ischemic microvascular perfusion. *J Neurochem* 2008;107:241–252.
18. Onyszczuk G, Al-Hafez B, He YY, *et al*. A mouse model of sensorimotor controlled cortical impact: characterization using longitudinal magnetic resonance imaging, behavioral assessments and histology. *J Neurosci Methods* 2007;160:187–196.
19. Niego B, Horvath A, Coughlin PB, *et al*. Desmoteplase-mediated plasminogen activation and clot lysis are inhibited by the lysine analogue tranexamic acid. *Blood Coagul Fibrinolysis* 2008;19:322–324.
20. Sappino AP, Madani R, Huarte J, *et al*. Extracellular proteolysis in the adult murine brain. *J Clin Invest* 1993;92:679–685.
21. Ida N, Hartmann T, Pantel J, *et al*. Analysis of heterogeneous A4 peptides in human cerebrospinal fluid and blood by a newly developed sensitive Western blot assay. *J Biol Chem* 1996;271:22908–22914.
22. Nagai T, Yamada K, Yoshimura M, *et al*. The tissue plasminogen activator-plasmin system participates in the rewarding effect of morphine by regulating dopamine release. *Proc Natl Acad Sci USA* 2004;101:3650–3655.
23. Qian Z, Gilbert ME, Colicos MA, *et al*. Tissue-plasminogen activator is induced as an immediate-early gene during seizure, kindling and long-term potentiation. *Nature* 1993;361:453–457.
24. Yepes M, Sandkvist M, Coleman TA, *et al*. Regulation of seizure spreading by neuroserpin and tissue-type plasminogen activator is plasminogen-independent. [see comments.]. *J Clin Invest* 2002;109:1571–1578.
25. Liu RM, van Groen T, Katre A, *et al*. Knockout of plasminogen activator inhibitor 1 gene reduces amyloid beta peptide burden in a mouse model of Alzheimer's disease. *Neurobiol Aging* 2009 (in press).
26. Rogove AD, Lu W, Tsirka SE. Microglial activation and recruitment, but not proliferation, suffice to mediate neurodegeneration. *Cell Death Differ* 2002;9:801–806.
27. Lu W, Bhasin M, Tsirka SE. Involvement of tissue plasminogen activator in onset and effector phases of experimental allergic encephalomyelitis. *J Neurosci* 2002;22:10781–10789.
28. Seeds NW, Basham ME, Ferguson JE. Absence of tissue plasminogen activator gene or activity impairs mouse cerebellar motor learning. *J Neurosci* 2003;23:7368–7375.
29. Thewke DP, Seeds NW. The expression of mRNAs for hepatocyte growth factor/scatter factor, its receptor c-met, and one of its activators tissue-type plasminogen activator show a systematic relationship in the developing and adult cerebral cortex and hippocampus. *Brain Res* 1999;821:356–367.
30. Lijnen HR, Van Hoef B, Collen D. Influence of cyanogen-bromide-digested fibrinogen on the kinetics of plasminogen activation by urokinase. *Eur J Biochem* 1984;144:541–544.
31. Muller A, Glattard E, Taleb O, *et al*. Endogenous morphine in SH-SY5Y cells and the mouse cerebellum. *PLoS One* 2008;3:e1641.
32. Iyer AM, Zurulo E, Boer K, *et al*. Tissue plasminogen activator and urokinase plasminogen activator in human epileptogenic pathologies. *Neuroscience* 2010;167:929–945.
33. Tsirka SE, Gualandris A, Amaral DG, *et al*. Excitotoxin-induced neuronal degeneration and seizure are mediated by tissue plasminogen activator. *Nature* 1995;377:340–344.
34. Wu YP, Siao CJ, Lu W, *et al*. The tissue plasminogen activator (tPA)/plasmin extracellular proteolytic system regulates seizure-induced hippocampal mossy fiber outgrowth through a proteoglycan substrate. *J Cell Biol* 2000;148:1295–1304.
35. Lahtinen L, Lukasiuk K, Pitkanen A. Increased expression and activity of urokinase-type plasminogen activator during epileptogenesis. *Eur J Neurosci* 2006;24:1935–1945.
36. Mori T, Wang X, Kline AE, *et al*. Reduced cortical injury and edema in tissue plasminogen activator knockout mice after brain trauma. *NeuroReport* 2001;12:4117–4120.
37. Nagai N, De Mol M, Lijnen HR, *et al*. Role of plasminogen system components in focal cerebral ischemic infarction: a gene targeting and gene transfer study in mice. *Circulation* 1999;99:2440–2444.
38. Armstead WM, Cines DB, Higazie AA. Plasminogen activators contribute to age-dependent impairment of NMDA cerebrovasodilation after brain injury. *Brain Res Dev Brain Res* 2005;156:139–146.
39. Dietzmann K, von Bossanyi P, Krause D, *et al*. Expression of the plasminogen activator system and the inhibitors PAI-1 and PAI-2 in posttraumatic lesions of the CNS and brain injuries following dramatic circulatory arrests: an immunohistochemical study. *Pathol Res Pract* 2000;196:15–21.
40. Natale JE, Ahmed F, Cernak I, *et al*. Gene expression profile changes are commonly modulated across models and species after traumatic brain injury. *J Neurotrauma* 2003;20:907–927.
41. Hamann GF, Burggraf D, Martens HK, *et al*. Mild to moderate hypothermia prevents microvascular basal lamina antigen loss in experimental focal cerebral ischemia. *Stroke* 2004;35:764–769.
42. Yepes M, Sandkvist M, Wong MK, *et al*. Neuroserpin reduces cerebral infarct volume and protects neurons from ischemia-induced apoptosis. *Blood* 2000;96:569–576.
43. Rosenberg GA, Navratil M, Barone F, *et al*. Proteolytic cascade enzymes increase in focal cerebral ischemia in rat. *J Cereb Blood Flow Metab* 1996;16:360–366.
44. Kim JW, Lee SH, Ko HM, *et al*. Biphasic regulation of tissue plasminogen activator activity in ischemic rat brain and in cultured neural cells: Essential role of astrocyte-derived plasminogen activator inhibitor-1. *Neurochem Int* 2010.
45. Kingston IB, Castro MJ, Anderson S. *In vitro* stimulation of tissue-type plasminogen activator by Alzheimer amyloid beta-peptide analogues. *Nat Med* 1995;1:138–142.
46. Jacobsen JS, Comery TA, Martone RL, *et al*. Enhanced clearance of Abeta in brain by sustaining the plasmin proteolysis cascade. *Proc Natl Acad Sci USA* 2008;105:8754–8759.
47. Ledesma MD, Da Silva JS, Crassaerts K, *et al*. Brain plasmin enhances APP alpha-cleavage and Abeta degradation and is reduced in Alzheimer's disease brains. *EMBO Rep* 2000;1:530–535.
48. Cacquevel M, Launay S, Castel H, *et al*. Ageing and amyloid-beta peptide deposition contribute to an impaired brain tissue plasminogen activator activity by different mechanisms. *Neurobiol Dis* 2007;27:164–173.
49. Fabbro S, Seeds NW. Plasminogen activator activity is inhibited while neuroserpin is up-regulated in the Alzheimer disease brain. *J Neurochem* 2009;109:303–315.

50. Melchor JP, Pawlak R, Strickland S. The tissue plasminogen activator-plasminogen proteolytic cascade accelerates amyloid-beta (Abeta) degradation and inhibits Abeta-induced neurodegeneration. *J Neurosci* 2003;23:8867–8871.
51. Roussel BD, Macrez R, Jullienne A, *et al*. Age and albumin D site-binding protein control tissue plasminogen activator levels: neurotoxic impact. *Brain* 2009;132(Part 8):2219–2230.
52. Garcia-Alloza M, Robbins EM, Zhang-Nunes SX, *et al*. Characterization of amyloid deposition in the APP^{swe}/PS1^{dE9} mouse model of Alzheimer disease. *Neurobiol Dis* 2006;24:516–524.
53. Ruan L, Kang Z, Pei G, *et al*. Amyloid deposition and inflammation in APP^{swe}/PS1^{dE9} mouse model of Alzheimer's disease. *Curr Alzheimer research* 2009;6:531–540.
54. Zoghbi HY, Orr HT. Spinocerebellar ataxia type 1. *Semin Cell Biol* 1995;6:29–35.